International Journal of Engineering Sciences & Research Technology

(A Peer Reviewed Online Journal)
Impact Factor: 5.164

IJESRT

RESEARCHERID
THOMSON REUTERS

[DIOP * *et al.*, 7(12): December, 2018]
IC™ Value: 3.00

ISSN: 2277-9655
Impact Factor: 5.164
CODEN: IJESS7

IJESRT

INTERNATIONAL JOURNAL OF ENGINEERING SCIENCES & RESEARCH TECHNOLOGY

RESTITUTION OF ATMOSPHERIC MOISTURE FROM NEURAL NETWORKS AND USING SATELLITE DATA

Bouya DIOP
LABORATOIRE DES SCIENCES DE L'ATMOSPHERE ET DES OCEANS UNIVERSITE GASTON BERGER de Saint Louis SENEGAL

DOI: 10.5281/zenodo.2526199

ABSTRACT

In the Sahelian region of West Africa most of the population lives agro-pastoral activities. The air trafficking, which is a source of sustainable development of countries which constitute this climatic zone develops. Hence the need for a weather forecast in the short and medium term.
In this work, it is a question of trying to restore the humidity of the atmosphere using neural networks. The model of liebe associated modtran 6 with us allowed to establish profiles of radiances. These structures are compared to those of the satellite. We obtained satisfactory results on the humidity profiles.

KEYWORDS: Humidity, sahel, Satellite, neuronal networks, radiatif transfer.

1. INTRODUCTION

The history of formal neurons goes back to cybernetics, in the forties of the past, when biologists, physicists, mathematicians and engineers came together to try to simulate, using electronic components, biological, physical, or even social phenomena. In technical terms, formal neurons are automata that characterize, by a mathematical definition, what we imagined to be, at the time of cybernetics, the function of neurons in our brain, namely the memorization of information elementary binary.

Artificial neural networks are composed of simple elements (or neurons) operating in parallel. These elements were strongly inspired by the biological nervous system (Figure 1). As in nature, the functioning of the (neuron) network is strongly influenced by the connection of the elements to each other. We can train a neuron network for a specific task (character recognition for example) by adjusting the values of the connections (or weights) between the elements (neuron).

In general, the learning of the neural networks is done so that for a particular input presented to the network corresponds a specific target.

ISSN: 2277-9655
Impact Factor: 5.164
CODEN: IJESS7

Figure 1. **Nerve cells (neurons) with branches (dendrites) connected to more than 100 trillion points of connections. Scientists call this dense network of ramifications the "forest of neurons".**

This is the classification of clouds which received the first applications of neural networks in physics of the atmosphere [1]. Formal networks have indeed useful features for pattern recognition and image analysis. This is the approach taken by Lee et al. (1990) [2] for their classification, followed by work Welch et al. (1992) [3]and Bankert (1994) [4] and Bankert and Aha (1996) [5].

Then the generally non-linear responses of electromagnetic waves with geophysical parameters, justifying the increasing use of this inversion technique. For example, Krasnopolsky et al. (2000) [6], from a multi-channel approach, propose a neural network algorithm for ocean refunds based on SSM / I (surface wind speed, water vapor column, and liquid water column).

Rainfall also have obviously been many studies using neural networks. Tsindikis et al. (1997) [7] adopted the first this method with brightness temperatures and rain rate output of the network, generated by a 3D radiative transfer model and a stochastic 3D cloud model, with a generalization from the SSM / I data. In approaches at the regional level, various types of data were also used as rain gauges and radar data (Matsoukas et al., 1999) [8], or the combination of data on the PR rain radar and the GOES multispectral imaging (Bellerby et al., 2000) [9]. In this latest study, statistical information are co-located with precipitation measurements to incorporate information on the cloud texture. Chopin et al, (2004) [10] combine input their data network Meteosat, GOES and TRMM precipitation to recover the data from TRMM radar is also used as network outputs. In principle one can obtain a relationship between the rain rate the ground and radar observations. However, it is difficult to express it in the usual way. Neural networks provide a mechanism to solve this complex problem. Li et al. (2003) [11] using this technique and use measurements of rain rate as the target output of the network, and the radar data as input to find the surface rain rate. Networks are also used to find the LWC (liquid water content) over oceans (Jung et al., 1998[12]; Aires et al., 2001) [13] or to obtain vertical temperature profiles from radiometers MW data as the SSM / T1 (Churnside et al., 1994[14];. Bauer et al, 2005) [15] or a combination of MW and IR (Kuligowski and Barros, 2001) [16]

.

The signing of the microwave broadcast retrieves the surface parameters such as those related to snow (Davis et al., 1993) [17] or sea ice (Fuhrhop et al., 1998) [18]. Jones and Peterson (1999) [19] propose a method to render the ocean surface temperature. Labroue et al. (2003) [20] propose a method of surface salinity refund from SMOS brightness temperatures (Soil Moisture and Ocean Salinity). The inversion algorithm is improved when adding additional

ISSN: 2277-9655
Impact Factor: 5.164
CODEN: IJESS7

parameters such as the surface temperature or the speed of the wind surface. Kretzschmar et al. (2004) [21] using a classification neural network for prediction of surface wind speed. Faure et al. (2001a, b) [22], [23] and more recently Cornet (2003) [24] marked the beginning of refunds parameters derived from the IR / VIS as optical thickness, the effective radius, the fractional coverage or even heterogeneous sub-pixel (defined by the standard deviation of the optical thickness). They came into use neural networks, the multispectral reflectance from clouds generated by a multiplicative cascade process. The effects of heterogeneities on refunds precipitation from passive microwave was studied by Lafont [25]and quotes in 2004 and Lafont, O.jourdan Guillemet and Bernard [26]still in the same year (2004) using the network neurons.

Still in a satellite data inversion order to obtain meteorological parameters, neural networks will be for us a way to connect the microwave physical information and spatial information from sensors higher satellites resolution (or http://www.esa.int/export/esaLP/smos.html http://www.cesbio.ups-tlse.fr/us/indexsmos.html) [27].

The problem of non-linear inversion equation is solved by these networks as an optimization problem. The satellite data inversion procedure requires the use of a large number of data channels and containing sufficient information on the temperature and relative humidity to be recovered. To restore these settings by cloudy weather, we estimated, using atmospheres summer (between June and October in the Sahel). We have already shown in a previous study that the parameters do not present too great a degree of correlation. Correlation analyzes are given by the studies by B. Diop in 1995[28] then by B. Diop and A. Diop in 2007[29].

The neural network method used here allow us this inversion of satellite data. Neural methods are increasingly used in atmospheric physics (Krasnopolsky et al 2003a, 2003b) [30] [31] whether for the simulation of complex processes or some rendering issues. These techniques have advantages for some of the problems encountered in atmospheric sciences: they can approach the complex functions of several variables without knowing the exact form of these functions (Denison et al., 2002) [32]; they are fast, flexible if the problem at hand has been well analyzed (Cheng and Titterington, 1994) [33].

2. MULTILAYER PERCEPTRON

The multilayer perceptron is a type of network most used neurons because it allows, through its many connections, performing nonlinear associations between two vectors.
A neuron has N inputs and one output (Figure 2). Each entry is associated with a wireless weight. The first operation performed is a weighted sum of the weight vector W of the input data, to which is added a bias b. is thus obtained, if X represents the N components of the input vector

$$a = \sum_{i=1}^{N} W_i X_i + b_i$$

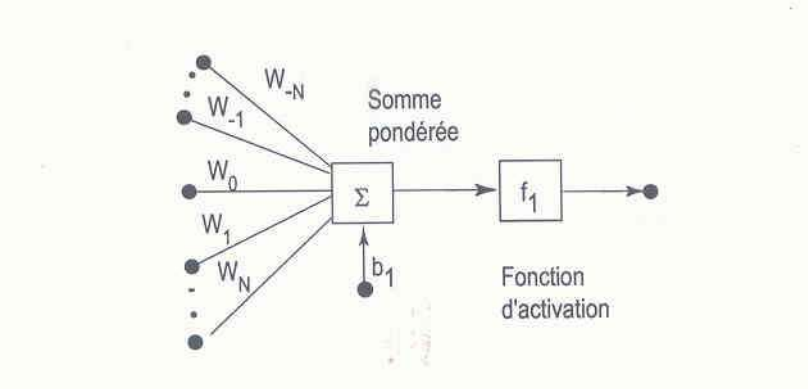

Figure 2. **General model of the formal neuron**

To this sum is then applied a feature called f_1 or activation function neuron function. Different functions can be applied, their choice depends on the complexity of the network that is used; may be (i,ii,iii,iv)

-
-
-

ISSN: 2277-9655
Impact Factor: 5.164
CODEN: IJESS7

- Linear Functions :

- $Y = \alpha a + \beta$ avec α et β (i)

- Shreshold funtions :

- $$Y = \begin{cases} 1, si\ a \geq \theta \\ -1,\ si\ \leq \theta \end{cases}$$ (ii)

- Sigmoid Functions : $Y = \frac{2}{(1+e^{-2a})-1}$ (iii)

- The output $Y = f(\sum_{i=1}^{N} W_i X_i + b_i)$ (iv)

A multilayer perceptron (Figure 3) is composed of an assembly of neurons distributed over L layers. The first layer corresponding to the vector composed of the input data and the last layer output vector composed of the values which it is desired to obtain. In between, there are a number of layers "caches". The complexity of the network depends on the number of hidden layers and the number of elementary neurons each component layer.

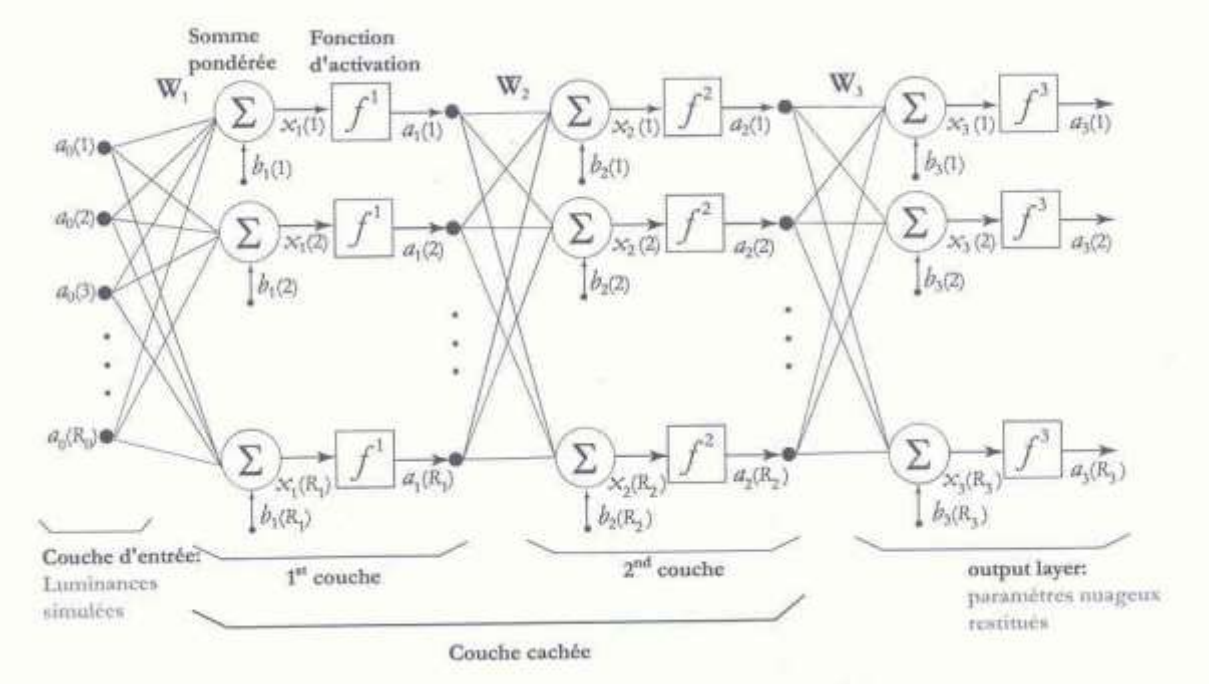

Figure 3 multilayer perceptron

3. USING NEURAL NETWORKS

The neural network is a type of parametric model that creates a nonlinear association between inputs and outputs. To achieve this combination, the different network coefficients must be adjusted. This adjustment is performed by minimizing the differences between the calculated outputs corresponding to the known input and the true output values. Once the examples have allowed the adjustment of the coefficients of the network, a test phase is required to evaluate the network performance. The use of neuronal methods thus breaks down into three phases:

Construction based learning, that is to say obtaining input-output pairs;
Neural network learning that corresponds to the adjustment of the various coefficients of the neural network;
Generalization phase of evaluating the performance of the neural network using data that were used during the learning phase.

ISSN: 2277-9655
Impact Factor: 5.164
CODEN: IJESS7

4. BULDING OF THE LEARNING BASE

The construction of the training base is the key step for the proper functioning of the networks. The data should be representative of a maximum possible situations because a well constructed neural network has very good interpolation properties but can also lead to large errors when it must extrapolate (Krasnopolsky and Schiller, 2000; 2003a) [34] [35]. this is why it appears preferable to use synthetic data that control the range of variation of the different parameters and thus to take into account extreme situations that may not exist a measured data set . The radiative transfer model used for the simulation data must correspond better to the actual measurements for the learning network is not biased by the learning model.

5. LEARNING NEURAL NETWORKS

Once built the base data, input vectors and associated target vectors are present in the neural network to allow adjustment of network coefficients (THIRIA et al., 1997) [36]. For an input vector $\{\vec{X} = (x_n); n = 1,..., N\}$, learning is to minimize the difference between the output given by the neural network $\{\vec{s} = (s_m); m = 1,..., M\}$ and the desired output $\{\vec{t} = (t_m); m = 1,..., M\}$> RE cost function of the empirical risk is often minimize the mean square error, W * coefficients are determined by minimizing RE (v)

$$R_E = \frac{1}{M}\sum_{i=1}^{M}(t_i - s_i)^2 \qquad \text{(v)}$$

To perform this minimization, the method used "back propagation of the error gradient" (or "backpropagation"). The basic idea is that at any point W, the gradient vector of the empirical risk fatou points in the direction of the growing empirical risk. To decrease fff simply move in the opposite direction of the gradient .gamma. This is an iterative algorithm of changing the weight vector wi of the ith layer in iteration k according to (vi):

$$W_i(k+1) = W(k) + \nabla W_i(k) \qquad \text{(vi)}$$

Where $\nabla W_i(k)$ is proportional to the gradient of the opposition (vii):

$$\nabla W_i(k) = -\left(\frac{\partial^2 R_E(k)}{\partial^2 W_i}\right) \qquad \text{(vii)}$$

It is possible to use a method of Newton-type (viii):

$$\nabla W_i(k) = -\left(\frac{\partial^2 R_E(k)}{\partial^2 W_i}\right)^{-1}\left(\frac{\partial R_E(k)}{\partial W_i}\right) = H^{-1}(k)g(k) \qquad \text{(viii)}$$

Where H is the Hessian matrix and the gradient vector g..

To accelerate the convergence of the minimization, the Hessian matrix is expressed as a function of the Jacobian matrix J (matrix of the first derivatives) by $H = J^T J$ and the gradient vector $g = J^T e$ with e the vector of network errors.The Levenberg-Marquardt algorithm we chose, used as approximation for the Hessian matrix:(ix)

$$\Delta W_i(k) = -\left[J^T J + \mu I\right]^{-1} J^T e \qquad \text{(ix)}$$

Where μ is the adjustment parameter.

ISSN: 2277-9655
Impact Factor: 5.164
CODEN: IJESS7

When zero, the method returns to a Newton-type method using the approximation of the Hessian matrix. When μ at a great value, this method corresponds to a method of lowering the error gradient is with no small learning.

In fact, μ adjusts the learning step on each iteration, it decreases whenever the result of the objective function is improved (the learning step increases, which accelerates the convergence).

Estimating the G function to connect the inputs and outputs from a small number of data D, is an "ill-posed" problem in the sense of minimizing the empirical standard deviation exists but is not unique (THIRIA et al., 1997) [37]. A regularization method can transform evil into good problem poses problem posed by imposing constraints.

6. REGULARIZATION WITH THE BAYESIAN APPROACH

The classical regularization methods add a penalty term to the function of costs which can result eg:

- By penalizing heavy weights (x)

$$\lambda \sum_j W_j^2 \quad \text{(x)}$$

- By penelizing large and small weights (Weigend et al, ; 1991) (xi) :

$$\lambda \sum_j \frac{W_j^2}{1+W_j^2} \quad \text{(xi)}$$

With Bayesian formalism [38,39,40,41]., weights and bias are assumed to be random variables with specific probability distributions. Learning of the neural network is to determine the probability distribution of weight knowing the training data are attributed to weight a priori probability fixed and once the training data were observed, this is a priori probability transformed into probability postiori through the Bayes theorem. If D represents the set of learning data, P (W) the a priori probability density function of the weight, P (D / W) of the probability density of observed data knowing the weight of the networks and P (D / W) to postiori the probability that one seeks to determine the Bayes theorem is (xii):

$$P(W/D) = \frac{P(D/W)P(W)}{P(D)} \quad \text{(xii)}$$

For example, it is assumed a priori weight distribution, Gaussian, such that (xiii):

$$P(W) = \frac{\exp\left[-\frac{1}{2}\lambda W_i^2\right]}{Z_m(\lambda)} \quad \text{(xiii)}$$

ISSN: 2277-9655
Impact Factor: 5.164
CODEN: IJESS7

Where λ then the parameter chosen to minimize the probability postiori and $Z_W(\lambda)$ is a normalization constant depending only λ.

All examples presented to the neural network during the learning phase will obviously contains not all actually observable examples. Assuming that all unobservable inputs has a Gaussian shape centered on O and σ^2 variance, then it is shown that (xiv):

$$P(D/W) = \frac{\exp\left[-\frac{1}{\sigma^2}\sum_i (t_i - s_i)^2\right]}{Z_D(\sigma)} \quad \text{(xiv)}$$

Posteriori probability is thus written (xv):

$$P(D/W) = \frac{\exp\left[-(\frac{1}{\sigma^2}\sum_i (t_i - s_i)^2 + \frac{1}{2}\lambda W_i^2)\right]}{Z_W(\lambda) + Z_D(\sigma)} = \frac{\exp[-M(W)]}{Z_M(\lambda, \beta)} \quad \text{(xv)}$$

Maximize the probability a posteriori is therefore to minimize the amount M (W) can be rewritten (xvi):

$$M(W) = \frac{1}{\sigma^2} R_E - \lambda \ln[P(W)] \quad \text{(xvi)}$$

This equation can be interpreted as a cost function with penalty as function of the logarithm of the a priori weight distribution.

Generalization phase

The generalization phase is to test whether learning of the network is done correctly. To perform this test, input vectors which have been used in the learning phase is presented to the neural network. The gap must be obtained weak. In general, the database used is randomly separated into two parts: one part is used for learning and generalization for the second phase. Several reasons can be learned that the network gives poor results:

Quite simply, the neural network input data did not provide enough information to approach the desired output. The network is not complex enough for the type of approach desired function, in this case, simply increase the number of hidden layers and the number of neurons per layer.

It is in a case of over-fitting is to say that the neural network is able to perfectly calculate the output vector for the input vectors used for learning but not capable of processing data unknown. This suggests that the number of examples used was too high or the network architecture is too complex for the problem to treat. The baseyienne approach developed by Mackay (1992) and improved by Neal (1996) avoids this scenario because the simplest models are favored over complex models by the regularization term. The initialization of the network coefficients to or different stages of minimization do not allow the network to converge. This feature depends on the data set used and the order in which the examples are presented for learning. To work around this last

ISSN: 2277-9655
Impact Factor: 5.164
CODEN: IJESS7

problem, we will make several cases for learning and giving the network the lowest generalization error phase will be retained.

7. CONSTRUCTION OF THE DATABASE

For learning neural networks, we must have a representative as possible database. It must contain the target parameters of the neural network (meteorological parameters) and corresponding data (luminance at different levels and different wavelengths).

Data

We built our database from Dakar-Yoff radiosonde and satellite data we used the data provided by the orbits LERG

We extracted MSU radiances orbits are the center frequencies are given in Table 1 NOAA 14 from MetOffice AAPP software responsible for processing the orbits of the NOAA KLM.

Table 1. Channels MSU MSU sounder which measures radiation in the field of microwave to calculate atmospheric moisture profiles.

Channels MSU	1	2	3
Fréquencies (GHz)	50.31	53.73	54.96
Levels (hPa)	1010	700	300

At frequencies given in Table 1 are associated weight functions in Figure 4

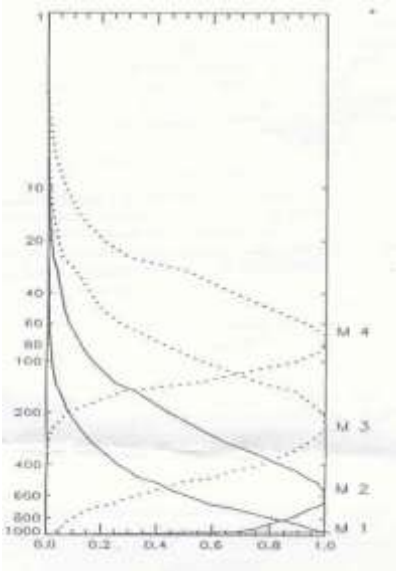

Figure 4. Weight function (MSU).

The weight functions for instrument MSU show that the energy contribution for each instrument channel from a considerable thickness atmosphere with a significant overlap between adjacent channels. Each channel represents a layer rather than a specific level.

The NOAA HRPT data is acquired in teaching Laboratory and Research in Geomatics (LERG, ISRA / UCAD) and presented in Table 2.

ISSN: 2277-9655
Impact Factor: 5.164
CODEN: IJESS7

Table 2. The NOAA HRPT data is acquired LONG (ISRA / UCAD).
Column 1: orbit number; Column 2: transition date on the study area, column 3: Passage Time (recording); column 4: the satellite track with geographic coordinates; Column 5: synoptic of the atmosphere.

Sat Orb	Date	Hour	Trace Zone	Notes
1413782	970902	40745	C.Vert 33N -> 3N	
1413788	970902	151951	W Dakar 2S -> 27N	
1413796	970903	35635	E C.Vert 32N -> 3N	S.L south senegal
1413802	970903	150937	Dakar 1N -> 27N	
1413810	970904	34557	W Dakar 30N -> Eq	
1413816	970904	145837	Sénégal 1N -> 30N	Covered
1413824	970905	33454	W Dakar 30N -> Eq	Covered
1413830	970905	144650	Mauritanie Eq -> 33N	
1413838	970906	32305	Senegal 32N -> 4S	
1413852	970907	31210	Bamako 31N -> 4S	S.L North Senegal
1413866	970908	30210	Mali 27N -> 3N	
1413880	970909	25039	Mali 28N -> 3N	
1413887	970909	154541	C.Vert 4N -> 25N	
1413894	970910	24037	Mali 26N -> 1N	S.L South east Senegal
1413901	970910	153333	E C.Vert Eq -> 28N	
1413909	970911	141011	C.Vert 30N -> 3N	S.L on Senegal
1413915	970911	152227	W Dakar Eq -> 30N	Covered
1413923	970912	35924	C.Vert 29N -> 3N	Covered
1413929	970912	151141	Dakar 3N -> 33N	
1413937	970913	34813	W Dakar 29N -> Eq	
1413943	970913	150011	Sénégal Eq -> 29N	
1413951	970914	33706	Sénégal 29N -> 8N	
1413971	970915	143908	Mauritanie 6N -> 36N	
1413979	970916	31530	E Sénégal 27N -> Eq	
1413985	970916	142900	Mauritanie 9N -> 38N	
1413993	970917	30328	Bamako 30N -> 3N	
1414028	970919	153638	C.Vert 4N -> 28N	
1414042	970920	152546	W Dakar 6N -> 22N	Covered
1414050	970921	40039	C.Vert 30N -> 3N	
1414056	970921	151406	Dakar 3N -> 30N	
1414070	970922	150211	Sénégal 1N -> 29N	
1414078	970923	33917	Dakar 27N -> Eq	
1414084	970923	145148	Bamako 4N -> 30N	
1414092	970924	32805	E Dakar 27N -> Eq	
1414098	970924	144116	Mauritanie 6N -> 36N	
1414106	970925	31732	Sénégal 26N -> Eq	S.L Senegal
1414112	970925	143010	Mauritanie 7N -> 37N	Covered

ISSN: 2277-9655
Impact Factor: 5.164
CODEN: IJESS7

1414163	970929	41315	E C.Vert 31N -> 4N	Covered
1414169	970929	152647	W Dakar 3N -> 30N	
1414177	970930	40301	C.Vert 28N -> 3N	Covered
1414183	970930	151511	Dakar 1N -> 33N	S.L South Senegal

The radiance data calculated

The radiance data calculated (Figures 5; 6; 7; 8) are obtained using the MPM93 Liebe code that we modified. On calculates the radiance of an atmosphere in the field of microwave several pressure levels.

A program calculates the weighting functions and brightness temperatures for microwave frequencies of 1 to 1000 GHz. The meteorological variables (height, pressure, temperature, air density, water vapor and aerosols) and emissivity constitute the inputs of the code for obtaining the radiance profile of the atmosphere. In Figure 5 we have the means of composite profiles radiances calculated using radiosonde has carried out two hours before the SL passages we note we have a maximum around 700 hPa to 50.31 GHz and 53.73 GHz channels except for profile 54.96 radiance of the channel. For the channel is a maximum to 800 hPa.

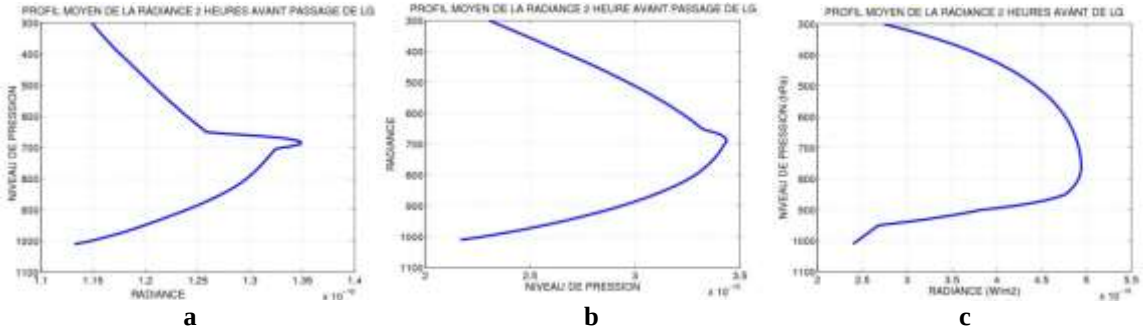

a **b** **c**

Figure 5. Average profile of Radiance 2 hours before the passage of squall line (SL)
a) 50.31 GHz ; b) 53.73GHz ; c) 54.96 GHz

In Figure 6 we have the composition of the average profiles radiance with soundings made the passage of SL we note we have a maximum at about 600 hPa. A slight variation of the radiance between 800 hPa and 450 hPa. The radiance profile 54.96 GHz channel we have the maximum at 500 hPa and a slight variation of the radiance between 800 hPa and 500 hPa.

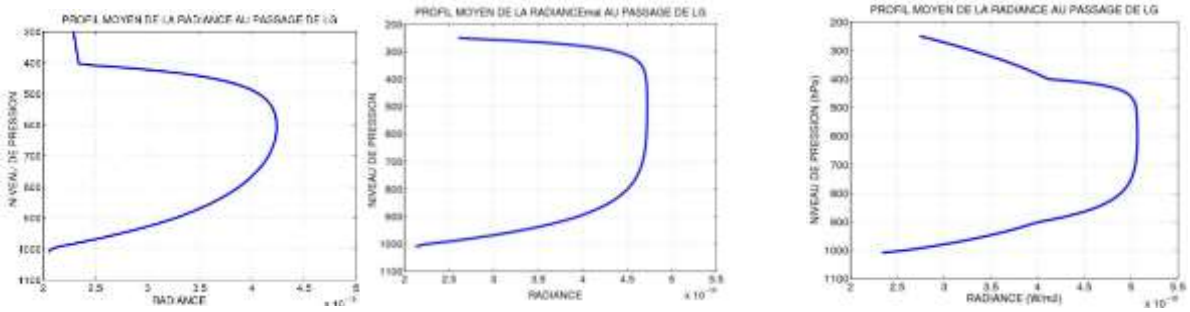

a **b** **c**

Figure 6. Average profile of Radiance at the passage of squall line
a) 50.31 GHz ; b) 53.73z ; c) 54.96 GHz

In Figure 7 the composition we mean profiles radiances using radiosonde performed at 2 hours after the passage of SL We note we have a maximum 700hPa to 50.31 GHz for channel and a relatively marked change in radiance between 1000hPa and 700hPa. The radiance profile channel as 53.73 to 54.96 GHz channel we have

ISSN: 2277-9655
Impact Factor: 5.164
CODEN: IJESS7

the maximum at 400hPa. We also note a slight change in radiance between 800hPa and 400hPa 53.73 for the channel and the same between 800hPa and 500hPa to 54.96 GHz channel.

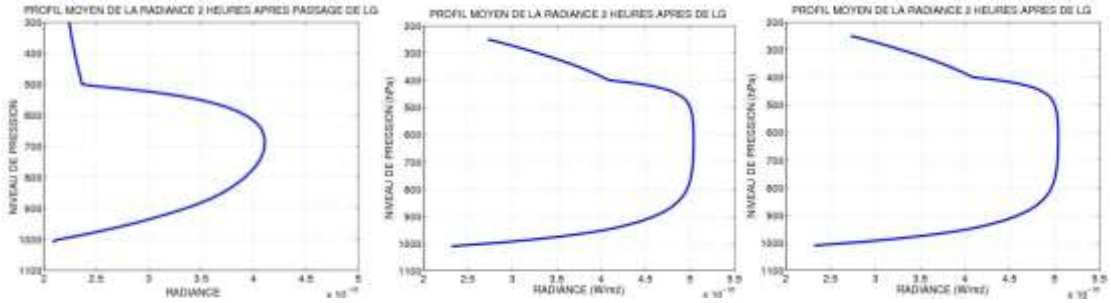

a **b** **c**

Figure 7. Average profile radiance two hours after the passage of SL
a) 50.31 GHz ; b) 53.73z ; c) 54.96 GHz

In Figure 8 we have the composition means profiles radiances with radiosonde performed at 4 hours after the passage of SL We note we have a maximum to 700hPa for channel 50.31 GHz and a relatively marked change in radiance between 1000hPa and 700hPa . The radiance profile shows a channel 53.73 maxima at 650hPa. 54.96 GHz for channel we have the maximum at 400hPa. We also note a slight change in radiance between 800hPa and 600hPa to 54.96 GHz channel.

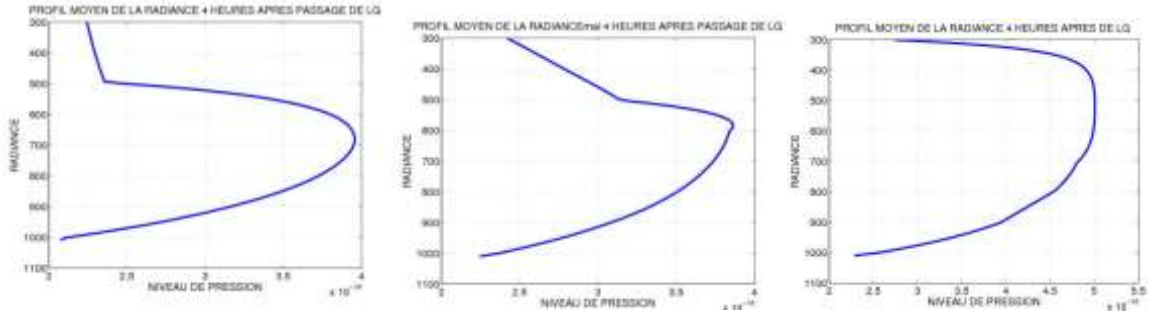

a **b** **c**

Figure 8. Average profile radiance four hours after the passage of squall line (SL)
a) 50.31 GHz ; b) 53.73z ; c) 54.96 GHz

We see differences between the vertical profiles of the atmosphere means for radiance. These differences are due to the position of surveys internally convective type SL systems

8. RESULTS ANALYSIS

Although the most difficult problem is the inversion of the radiative transfer equation, it is important to have a fast direct model, for the basic construction of data. The Liebe MPM93 modified code has been developed for this purpose at LSAO.

Analyse de l'apprentissage Learning analytics

We therefore tested the ability of neurons to the forward model network, that is to say that we present at the input of the neural network state temperature profiles, brightness temperatures calculated by the model, levels pressure and the geo-potential altitude and that it is desired to restore moisture to the atmosphere. For this test all three channels (50.31, 53.73, 54.96) MSU are taken into account.

The architecture used is the following:

- Input: temperature profiles of 11 pressure levels;
- Water vapor profiles in 11 steps;
- Air density profiles of 11 levels.

ISSN: 2277-9655
Impact Factor: 5.164
CODEN: IJESS7

We on the first hidden layer neurons 20 and the second hidden layer neurons 20 also. Learning neural networks has been performed using the three spectral radiances (50.31 GHz; 53.73z; 54.96 GHz) at the levels of pressure observation scale, the atmosphere temperatures and levels geopotential. Learning is made from convective atmosphere SL influence described in Chapter 2. The input vector to the network is made up of geopotential height, pressure level, the value of the survey channel radiance expressed in brightness temperature and specific humidity (we want to restore). Learning neural networks shall be effected from 6666 results Entries vectors are present in Figure 9. Figure 9a shows the parameters during the learning neural network. Learning stopped after 1112 iterations, because the increased validation error. This is a useful diagnostic tool to trace the training errors, validation and test to check the progress of learning. Figure 9B shows that the Bayesian regularization, which assumes that the weights and biases follow specific distributions (parameters are estimated as and learning) generally gives very satisfactory results. Figure 9 shows comparisons among returned parameters (Outputs) by the network of neurons and initial parameters (Target). Network outputs are plotted against the target open circles. The best linear fit is indicated by a dotted line. The perfect fit (output equal to the target) is indicated by the solid line. In the figure, it is difficult to distinguish the best linear fit line of the curve perfect fit, because the fit is so good. We have two exits, so we conducted two regressions. The results are shown in Figure 9C, D. These two outputs Figure 9C, D, seem to follow the targets reasonably well, and R values are close to 0.9.

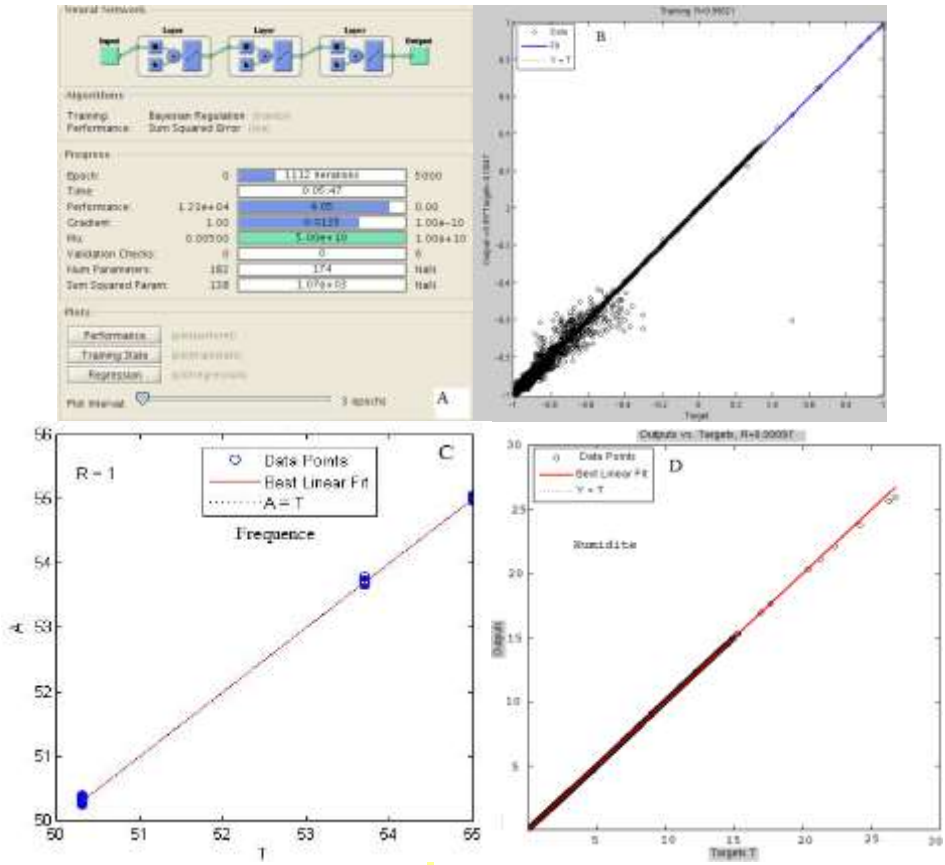

Figure 9. Learning Network

ISSN: 2277-9655
Impact Factor: 5.164
CODEN: IJESS7

Analysis of inverted data

We applied the restitution procedure in a summer atmosphere with the presence or absence of convective systems surveyed by the TOVS NOAA 14. Values are expressed in radiance shine temperatures for 50.31 GHz channels 53.73GHz, 54.96 GHz. The results obtained are presented in Figure 5.10. and tables (3-9).

In Figure 10, specific humidity is converted to relative humidity. The observed patterns are the average obtained from the radiosonde Dakar over the period 1968 -2006. Average monthly radiosonde is that of the month of September 1997.

The monthly average of the refund is the average taken from the orbits of September 1997. It was found that the monthly average for the return is close to the monthly average of radiosondes in the lower levels. For level 300 hPa, the values are more distant.

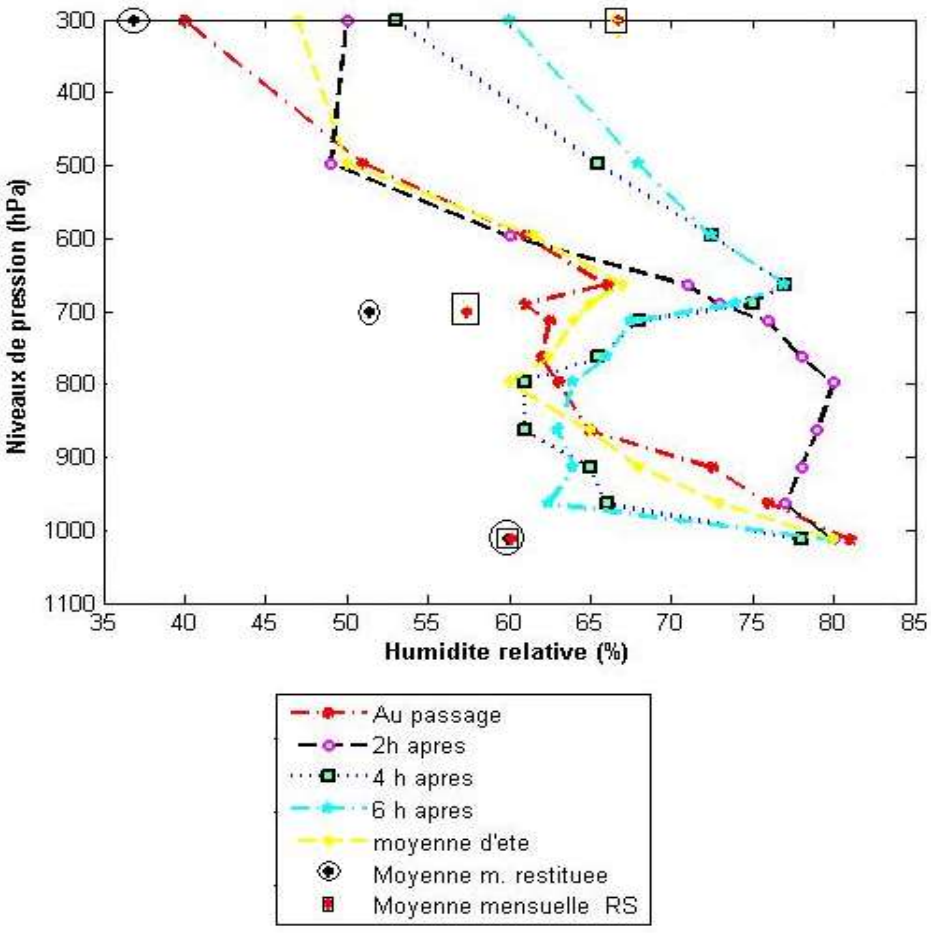

Figure 10. Profile of moisture restored compared to average summer humidity.

Table 3. Monthly average restitution of specific humidity (September 1997).

Levels	retrieval	RS: Monthly Average	Summer average (1968-2006)
1012	17.20	17.33	20.96
700	6.11	6.53	6.99
300	0.32	0.38	0.35

Note that monthly average is almost close to the average obtained by radiosonde in this climate zone.

ISSN: 2277-9655
Impact Factor: 5.164
CODEN: IJESS7

Table 4. The return of specific humidity to orbit 1413788 of September 2, 1997 at 3:19 p.m. obtained minutes and 51 seconds.

Levels (hPa)	retrieval	RS network of 12-hour	RS: Monthly Average	Summer average
1011	16.41	17.62	17.33	20.96
700	5.84	6.83	6.53	6.99
300	0.21	0.66	0.38	0.35

Table 5. The return of specific humidity to orbit 1413788 of September 3, 1997 at 3:09 p.m. obtained minutes 37 seconds

Levels (hPa)	retrieval	RS network of 12-hour	RS: Monthly Average	Summer average
1012	15.18	16.58	17.33	20.96
700	6.29	6.64	6.53	6.99
300	0.4	0.59	0.38	0.35

Table 6. the return of specific humidity to orbit 1413788 of September 11, 1997 obtained from 22 O'clock 27 minutes 51 seconds

Levels (hPa)	retrieval	RS network of 12-hour	RS: Monthly Average	Summer average
1012	18.57	16.77	17.33	20.96
700	7.63	7.76	6.53	6.99
300	0.8	0.04	0.38	0.35

Table 7. The return of specific humidity to orbit 1413788 of September 20, 1997 at 3:25 p.m. obtained minutes 46 seconds.

Levels (hPa)	retrieval	RS network of 12-hour	RS: Monthly Average	Summer average
1010	20.1	19.12	17.33	20.96
700	9.01	10.26	6.53	6.99
300	0.1	0.72	0.38	0.35

Table 8. The return of specific humidity to orbit 1413788 of September 25, 1997 obtained 3:17 minutes 32 seconds.

Levels (hPa)	retrieval	RS network of 12-hour	RS: Monthly Average	Summer average
1010	20.8	19.8	17.33	20.96
700	7.3	6.4	6.53	6.99
300	0.5	0.26	0.38	0.35

Table 9. The restitution of the specific humidity for the orbit 1413788 of September 30, 1997 obtained at 15 hours 15 minutes 11 seconds. retrieval ***of the specific humidity for the orbit 1413788 of September 30, 1997 obtained at 15 hours 15 minutes 11 seconds.***

Levels (hPa)	retrieval	RS network of 12-hour	RS: Monthly Average	Summer average
1010	16.44	16.67	17.33	20.96
700	6.67	7.33	6.53	6.99
300	0.4	0.05	0.38	0.35

These orbits were chosen because corresponding to atmospheres where one notes the presence of convective systems.

Radiative transfer codes that we used and modified MODTRAN MPM-Liebe, have allowed us to confrontations with satellite observations. In this chapter we have presented a method for reversing the equation of radiative transfer based on the technique of neural networks in retro error propagation. The results on simulated data for the inversion of MSU data are generally very good. This technique (neural network) was also applied to the fast modeling radiative transfer problem and the method of composite analysis shows a low minimization results especially at 300hpa. The method is especially highlighted an ability to simulate the channels probing the concentration of the variable component as atmospheric water vapor, which is a highly nonlinear problem, and therefore poorly understood by the conventional approach linearization around an approximate solution. Other significant advantages of this technique are:

- The low computing time use;

ISSN: 2277-9655
Impact Factor: 5.164
CODEN: IJESS7

- The reduction of several orders of magnitude the number of storing information for the algorithm.

The major drawback is the low algorithm convergence speed (the neural network) during the learning phase, which involves the use of long calculation means for this type of application. Comparisons with the calculations made from radiances and radiosonde measurement data with NOAA 14 allowed us to open a path to satellite survey convective troposphere atmosphere in the Sahel region. The advent of pollsters point to a significant gain in quality of restitution.

9. CONCLUSION

In the Sahelian region of West Africa most of the population lives agro-pastoral activities. The air trafficking, which is a source of sustainable development of countries which constitute this climatic zone develops. Hence the need for a weather forecast in the short and medium term.

There is a virtual absence of tropospheric radiosonde station in the Sahelian zone and the coastal area of West Africa in the summer. The numerical simulation of the atmosphere Sahelian solutions cover and "satellite surveys are to promote. The aim of this work is to characterize the atmosphere under the influence of convective systems line type of grain to the earth-sea interface. Squall lines produce essential rainfall in the Sahel. This work allowed the validation of numerical weather prediction models on the one hand, the other to validate the return of meteorological parameters derived from satellite sounders.

The modeling of the energy balance of the atmosphere with the convection necessarily requires consideration of radiative transfer. This work has enabled the development of radiative transfer models, coupled with satellite observations for a comprehensive study of changes in convective systems. Indeed, it has been shown that satellite dimension is essential in any study of the troposphere in this climate zone.

In general, part of the study included deep convection in the Sahel from the radiative energy balance using satellite data surveys. In practice, it is current NOAA-TOVS-ATOVS, radiosonde available in the area and re analysis NCEP / NCAR. A composite analysis followed by statistical processing, were used to compare the dynamic calculated fields to the measured radiance.

The first studies we have conducted on this topic, were made with LOWTRAN. MODTRAN an improvement compared to the simple diffusion. Compared to results of calculations with this code, it is important to note that the profiles of radiance obtained vary according to the poll position that one is in convective part (up to two hours after the detection of the SL) or stratiform SL. The spectral signatures of the atmosphere reveals a significant gap structures obtained in the comparison of atmospheric diffusion flows for the different time classes. Radiative transfer codes that we used MODTRAN and MPM-Liebe [42]. modified allowed us to confrontations with satellite observations. We used a method of inverting the radiative transfer equation based on the technique of back propagation of the error to neural networks. The results on simulated data for the inversion of MSU data are generally very good. This technique has also been applied to the problem of modeling and rapid calculation of radiative transfer and the method of composite analysis shows a low minimization results especially at 300 hPa. The method is especially highlighted an ability to simulate the channels probing the concentration of the variable component as atmospheric water vapor, which is a highly nonlinear problem, and therefore poorly understood by the conventional approach linearization around an approximate solution. Other important advantages of this technique are, firstly, the low computation time in use, on the other hand the reduction of several orders of magnitude the number of storing information for the algorithm. The major drawback is the low speed of convergence of the algorithm during the learning phase, which involves the use of long calculation means for this type of application. With comparisons between the

radiosonde measurements and measurement data with NOAA 14 allowed us to open a path to satellite survey convective troposphere atmosphere in the Sahel region. The advent of sounders and improving fast calculations of the equation of radiative transfer point to a significant gain in quality of restitution. This climatological cleared over several years of meteorological parameters of this climatic zone is a boon offered to operational forecasters West African meteorology and researchers from the world of physics of the atmosphere.

ISSN: 2277-9655
Impact Factor: 5.164
CODEN: IJESS7

REFERENCES

[1] Lafont, D., and B. Guillemet, 2004a: Subpixel fractional cloud cover and inhomogeneity effects on microwave beam-filling error, Atmospheric Research, 72, 149-168
[2] **Lee, J., R. C. Weger, S. K Sengupta, R. M. Welch, 1990:** A neural network approach to cloud classification, IEEE Trans. Geosci. Rem. Sens., 28, 846-855.
[3] Welch J.M., A.D. Little and P.R Nayak, 1992. Strategic Sourcing: A progressive approach to make or buy decision. Academy Of Management Executive, vol. 6, N°1, p. 23-31
[4] **Bankert, R. L., 1994:** Cloud classification of AVHRR imagery in maritime regions using a probabilistic neural network, J. Appl. Meteorol., 33, 909-918.
[5] **Bankert, R. L., D. W. Aha, 1996:** Improvement to neural network cloud classifier, J. Appl. Meteorol., 35, 2036-2039.
[6] **Krasnopolsky, V. M., W. H. Gemmill, L. C. Breaker, 2000:** A neural network multi parameter algorithm for SSM/I ocean retrievals: comparisons and validations, Rem. Sens. Env., 73,133-142.
[7] **Tsintikidis, D., J. L. Haferman, E. N. Anagnostou, W. F. Krajewski, T. F. Smith, 1997:** A neural network approach to estimating rainfall from spaceborne microwave data, IEEE Trans. Geosci. Rem. Sens., 35, 1079-1092.
[8] **Matsoukas, C., Islam, S., Kothari, R., 1998:** Fusion of radar and rain gage measurements for an accurate estimation of rainfall.Conference: 6th International Conference of Precipitation on Predictability of Rainfall at the Various Scales Location: MAUNA LANI BAY, HAWAII Date: JUN 29-JUL 01, Sponsor(s): Amer Geophys Union; Amer Meterol Soc; Mauna Lani Bay Hotel & Bungalows.
[9] **Li, W., V. Chandrasekar, G. Xu, 2003:** Investigations in radar rainfall estimation using neural networks, Proceedings International Geoscience and Remote Sensing Symposium, Toulouse, France.
[10] **Jung, T., E. Ruprecht, F. Wagner, 1998:** Determination of Cloud Liquid Water Path over oceans from Special Sensor Microwave Imager (SSM/I) data using neural networks, J. Appl. Meteorol., 37, 832-844.
[11] **Aires, F., C. Prigent, W. B. Rossow, M. Rothstein, 2001:** A new neural network approach including first guess for retrieval of atmospheric water vapor, cloud liquid water path, surface temperature, and emissivities over land from satellite microwave observations, J. Geophys. Res., 106, 14887-14907.
[12] **Churnside, J.H., Stermitz, T.A., Schroeder, J.A., 1994:** Temperature profiling with neural-network inversion of microwave radiometer data. Journal of Atmospheric and Oceanic Technology, 11, 105
[13] **Bauer, P., E. Moreau, S. Di Michele, 2005:** Hydrometeor retrieval accuracy using microwave window and sounding channel observations. J. Appl. Meteor., **44,** 1016–1032.
[14]
[15] **Bellerby, T., Todd, M., Kniveton, D., Kidd, C ., 2000:** Rainfall estimation from a combination of TRMM precipitation radar and GOES multispectral satellite imagery through the use of an artificial neural network . J. Appl. Meteorol.,39, 2115-2128.
[16] **Kuligowki, R. J., and A. P. Barros, 2001:** Combined IR-microwave satellite retrieval of temperature and dewpoint profiles using artificial neural networks, J. Appl. Meteorol., 40, 2051-2067.
[17] Yang, C. C., S. O. Prasher, and G. R. Mehuys, 1997: An artificial neural network to estimate soil temperature. Can. J. Soil Sci.,77, 421–429
[18] **Fuhrhop, R., T. C. Grenfell, G. Heygster, K. P. Johnsen, P. Schlüssel, M. Schrader, C. Simmer, 1998:** A combined radiative transfer model for sea ice, open ocean, and atmosphere, Radio Sci., 33, 303-316.
[19] **Jones, C., P. Peterson, C. Gauthier, 1999:** A new method for dériving ocean surface specific humidity and air temperature: An artificial neural network approach, J. Appl. Meteorol., 38, 1229-1245.
[20] **Labroue, S., E. Obligis, C. Boone, S. Philipps, 2003:** Salinity retrieval from SMOS brightness temperatures, Proceedings International Geoscience and Remote Sensing Symposium, Toulouse, France.
[21] **Kretzschmar, R., P. Eckert, D. Cattani, 2004:** Neural network classifiers for local wind prediction, J. Appl. Meteorol., 43, 727-738.
[22] **Faure, T., H. Isaka, B. Guillemet, 2001a:** Neural network analysis of the radiative interaction between neighboring pixels in inhomogeneous clouds, J. Geophys. Res., 106, 14465-14484.

ISSN: 2277-9655
Impact Factor: 5.164
CODEN: IJESS7

[23] **Faure, T., H. Isaka, B. Guillemet, 2001b:** Mapping neural network computation of high resolution radiant fluxes of inhomogeneous clouds, J. Geophys. Res., 106, 14961-14974.
[24] **Cornet, C., H. Isaka, B. Guillemet, and F. Szczap, 2004:** Neural network retrieval of cloud parameters of inhomogeneous clouds from multiscale radiance data: Feasability study, J. Geophys. Res., 109, D12203, doi: 10.1029/2003JD004186
[25] Lafont, D., and B. Guillemet, 2004b: Beam-filling correction with sub-pixel cloud fraction using a neural network, IEEE Trans. Geosci. Rem. Sens., accepté.
[26] Lafont, D., O. Jourdan, and B. Guillemet, 2004: Mesoscale cloud patterns classification over ocean with a neural network using a new index of cloud variability, Int. J. Rem. Sens., accepté.
[27] http://www.esa.int/export/esaLP/smos.html http://www.cesbio.ups-tlse.fr/us/indexsmos.html) .
[28] **Diop B., 2003:** Bilan hydrique Terre-Atmosphere au passage des ligne de grains à Dakar. Dokumentacja Geograpficzna,29, 81-84.
[29] **Diop B,** Diop A.,2006 : Analyse statistique des profils énergétiques radiatifs de l'atmosphère au passage des lignes de grains à Dakar ,), Proceeding ,XIX^{e} Colloque de l'Association Internationale de Climatologie, pp190-195. PRODIG, 2006, ISBN 2-9011560-70-9.
[30] **Krasnopolsky, V., Schiller, H., 2003:** Some neural network applications in environmental sciences. Part I: forward and inverse problems in geophysical remote measurements. Astronomy and geosciences, 16, 321-334.
[31] Yang, C. C., S. O. Prasher, and G. R. Mehuys, 1997: An artificial neural network to estimate soil temperature. Can. J. Soil Sci.,77, 421–429
[32] **Cheng, B., Titterington, DM,** 1994 [Réseaux de neurones: Un aperçu de la perspective statistique]: Réplique. Statist. Sci. 9, no. 1, 49-54. doi: 10.1214 / ss / 1177010646. https://projecteuclid.org/euclid.ss/1177010646
[33] **Cornet, C., 2003 :** Restitution de paramètres nuageux par méthodes neuronales dans des cas de nuages hétérogènes à couverture fractionnaire ; thèse d'université Blaise Pascal , 162pp ;
[34] **Krasnopolsky, V. M., W. H. Gemmill, L. C. Breaker, 2000:** A neural network multi parameter algorithm for SSM/I ocean retrievals : comparisons and validations, Rem. Sens. Env., 73, 133-142.
[35] **Kretzschmar, R., P. Eckert, D. Cattani, 2004**: Neural network classifiers for local wind prediction, J. Appl. Meteorol., 43, 727-738.
[36] **Lei SHI, 2000**: Retrieval of Atmospheric Temperature Profiles from AMSU-A Measurement Using a Neural Network Approach, JOURNAL OF ATMOSPHERIC AND OCEANIC TECHNOLOGY,8,340-347
[37] **Lee, J., R. C. Weger, S. K Sengupta, R. M. Welch, 1990:** A neural network approach to cloud classification, IEEE Trans. Geosci. Rem. Sens., 28, 846-855.
[38] **MacKay, D. J. C., 1992a:** Bayesian interpolation". Neural Computation, 4, 415-447.
[39] **MacKay, D. J. C. A.,1992b :** Practical Bayesian Framework for Backpropagation Networks. Neural Computation, 4, 448-472.
[40] **Neal, R. M., 1996:** Bayesian Training of Backpropagation Networks by the Hybrid Monte Carlo Method. Technical Report CRG-TR-92-1, Department of Computer Science, University of Toronto, 1992.
[41] **Neal, R. M., 1996:** Bayesian methods for Neural Networks. New York : Springer- Verlag,.
[42] **Liebe, H. J., G. A. Hufford, and M. G. Cotton, 1993:** Propagation modeling of moist air and suspended water/ice particles at frequencies below 1000 GHz, AGARD 52nd Specialist Meeting of the Electromagnetic Wave Propagation Panel, Brussels, Belgium, 3.1-3.10.

CITE AN ARTICLE

DIOP, B. (2018). RESTITUTION OF ATMOSPHERIC MOISTURE FROM NEURAL NETWORKS AND USING SATELLITE DATA. *INTERNATIONAL JOURNAL OF ENGINEERING SCIENCES & RESEARCH TECHNOLOGY, 7*(12), 330-346.